active K^{40}. Although the same radionuclides were reported in core samples from this general area (*6*), the *in situ* spectra are clearly superior. The large "sample size" assures an increased counting rate that more than compensates for the loss of detail resulting from the effects of the water on the γ-ray photons.

Comparison of a spectrum of coarse sand and gravel, in 30 m of water 1.6 km off Newport, Oregon (Fig. 2*b*), shows no radionuclides resulting from operations at the Hanford laboratories. The plume of the Columbia River does not normally move into this area, although marine animals taken here contain Zn^{65} (*7*). Most deposits of silts and clays in the northeast Pacific Ocean, which might have larger amounts of artificial radioactivity than sands and gravels, are beyond the present range of our probe. Range is restricted by the 54-m cable used in these tests, but Riel (*8*) has shown that longer cable lengths are feasible. The probe housing was designed for and tested at much greater pressures, and the only modifications required are in the cable length and associated electronics. These modifications are in progress and should let us work down to about 400 m.

Our interest lies in the relationship of the radioactivity of animals to that of their environment. Analysis techniques for animals are relatively simple, since the specific activity of the samples can be increased by ashing, with the ash counted in the well of a NaI(Tl) crystal (12.5 by 12.5 cm) in the laboratory. There is no easy comparable method of concentrating the radioactivity in sediment samples. The difficulties inherent in the collection and subsequent radioanalysis of sediments seem to make methods of probing *in situ* worthy of further effort.

DAVID JENNINGS
NORMAN CUTSHALL
CHARLES OSTERBERG
Department of Oceanography, Oregon State University, Corvallis

References and Notes

1. The actual depth to which the probe "sees" depends on both the energy of the γ-ray emitters and the density of the matrix material. Therefore, the effective size of the sample would be less for Cr^{51} (0.32 Mev) than for K^{40} (1.46 Mev).
2. J. H. Harley, Ed., *Operation* Troll: *Joint preliminary report* (HASL, U.S. Atom. Energy Comm., New York Operations Office, NYO 4656, April 1956).
3. C. M. Proctor, E. Papadopulos, R. H. Firminhac, *Limnol. Oceanogr.* **7**, 280 (1962).
4. M. G. Gross, C. A. Barnes, G. K. Riel, in preparation.
5. P. C. Klingeman and W. J. Kaufman, "Transport of radionuclides with San Francisco Bay sediments," Progress Report 1961-1962 Water Year. *Sanitary Eng. Res. Lab. Rep.* No. 63-7, (Univ. of California, Berkeley, 1963), p. 70.
6. C. Osterberg, J. Byrne, V. Kulm, *Science* **139**, 916 (1963).
7. C. Osterberg, J. Pattullo, W. Pearcy, *Limnol. Oceanogr.* **9**, 249 (1964).
8. G. K. Riel, *Electronics* **36**, No. 10, 56 (8 Mar. 1963).
9. Support from U.S. AEC contract AT(45-1)1750 and PHS training grant 1T1-WP-59-01. The data are a result of thesis research for a master's degree from Oregon State University. We thank R. S. Mesecar and W. E. Bales for design of the electronic circuitry and suggestions for waterproofing the probe.

23 February 1965

Kink-Bands: Shock Deformation of Biotite Resulting from a Nuclear Explosion

Abstract. *Microscopic examination of granodiorite samples from the shock region around a nuclear explosion reveals sharply folded lens-shaped zones (kink-bands) in the mineral biotite. Fifty percent of these zones are oriented approximately 90° to the direction of shock-wave propagation, but other zones are symmetrically concentrated at shear angles of 50° and 70° to the direction of shock-wave propagation.*

In 1962, a 5.2-kiloton nuclear device was detonated in the granodiorite of the Climax stock, Nevada Test Site (Hardhat event). Deformation of biotite in the form of sharply folded lens-shaped zones (kink-bands) was observed by microscopic examination of samples affected by the shot. As a basis for defining explosion-produced effects, samples taken prior to the detonation were examined and compared with those taken after the shot (postshot samples). The locations in the reentry tunnel where the postshot samplings were made and the drill core are shown in Fig. 1.

All thin sections cut from the six samples in the reentry tunnel were oriented by having the planar dimension of the section parallel to a radius drawn from the shot point. Although the orientation for most sections cut from the postshot drill core was not known (because of rotation of the sample in the core barrel during drilling), sections from the four samples C_8, C_9, C_{10}, and C_{11} could be oriented parallel to a radius from the shot point.

Of the ten oriented postshot sections only the eight within the shock zone (*1*) displayed kink-bands (Fig. 1). These eight were examined for preferred directions of kink-bands. Of the 110 observed kink-bands in the oriented sections, 50 percent were oriented with the long axis of the lens at 90° ± 5° to a radius drawn from the shot point (Fig. 2*A*). Approximately 12 percent and 10 percent were oriented with the long axis of lens at 50° ± 1° and 70° ± 1°, respectively, from the radius (Fig. 2*B*).

Because only the eight oriented samples within the shock zone showed kink-bands, the explosion-produced shock wave was probably the (compressive) stress which formed the kink-bands. The shock wave passes spherically outward from the shot point so that its front moves along radii drawn from the shot point. The kink-band orientation can thus be related to the direction of wave propagation. The unoriented sections can be oriented by assuming that the greatest percentage of kink-bands is normal to the direction of shock-wave propagation.

A total of 701 kink-bands from oriented and unoriented sections were counted. Their frequencies and orientations with respect to the shock wave are shown on Fig. 3. The relative frequencies of the principal orientations for the unoriented sections are the same as those from the oriented sections. This suggests that the method for deducing the direction of shock-wave propagation in unoriented sections is not greatly in error.

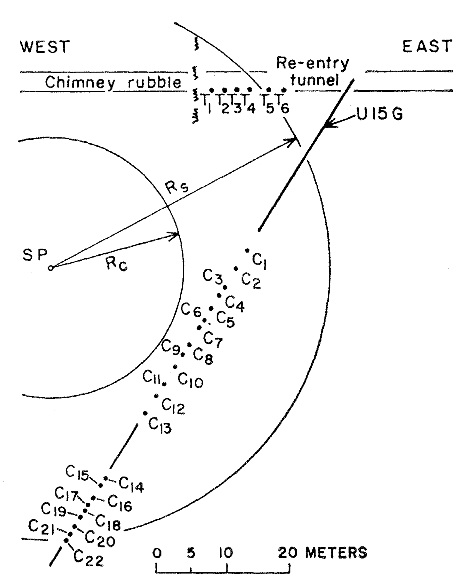

Fig. 1. Cross-sectional diagram in the vicinity of the Hardhat event showing the reentry tunnel, postshot drill hole (U15G), shock-zone radius (R_s), cavity radius (R_c), shot point (SP), and sample locations in the tunnel ($T_1 \cdots T_6$) and drill hole ($C_1 \cdots C_{22}$).

Figure 3 shows the greatest concentration of kink-bands with their long axes normal to the direction of shock-wave propagation. The second greatest concentrations of kink-bands are symmetrically disposed at angles of 50° and 70° to the shock-wave direction.

The orientation of kink-bands to compressive stress is illuminated by experimental work. Griggs, Turner, and Heard (*2*) showed that the long axis of kink-bands in biotite in an experimentally deformed granite tended to develop normal to the axis of compression. Paterson and Weiss (*3*), in experimental studies of phyllite, found conjugate sets of kink-bands symmetrically oriented at 50° to the direction of shortening in specimens compressed parallel to the foliation, but only one set developed in specimens compressed at 25° and 45° to the foliation. These laboratory studies suggest that orientations both normal and at a moderate angle to the axis of compression are possible as primary deformation features. Ramsey (*4*) suggested that a second-order shear, resulting from a rearrangement of the principal stress directions, accounts for the development of shear folds (similar to kink-bands).

These experiments (*2, 3*) might readily explain the concentrations at 90° and 50°. Neither experiment, however, explains the 70° concentrations. As suggested by Ramsey (*4*), it may be possible to explain the 70° concentrations as second-order shear.

McKinstry (*5*) and Moody and Hill (*6*) described the expected geometry of deformation resulting from a compressive stress. If the direction of the compressive stress (shock wave) is given with a primary shear angle at 50°, and if the "critical angle" (*6*) is set to 20°, the concentration at 70° may be explained as resulting from second-order shear (Fig. 4).

As stated above, it is believed that the shock wave (and, therefore, the stress) formed the kink-bands. Although the passage of the shock wave is supersonic (*7*), and the development of second-order shears requires some time for the redistribution of internal stresses, it nevertheless seems possible to argue that all the kink-bands resulted from a single primary stress—the shock wave.

Figure 5 qualitatively shows the passage of the shock wave from the detonation point, *0*, to the edge of the shock zone (R_s). The history of kink-band formation at a point may be related to the passage of the shock wave in time, distance, and peak compressive stress. The shock-wave front passes point *A* at time T_1, forming kink-bands normal to the direction of shock-wave propagation (90°) and primary shear sets (50°). The pressure behind the wave front does not return to ambient immediately after the passage of the front. For point *B* and time T_2, a similar argument can be proposed. At point *A* and time T_2, however, there is overpressure remaining which may be sufficient both in time

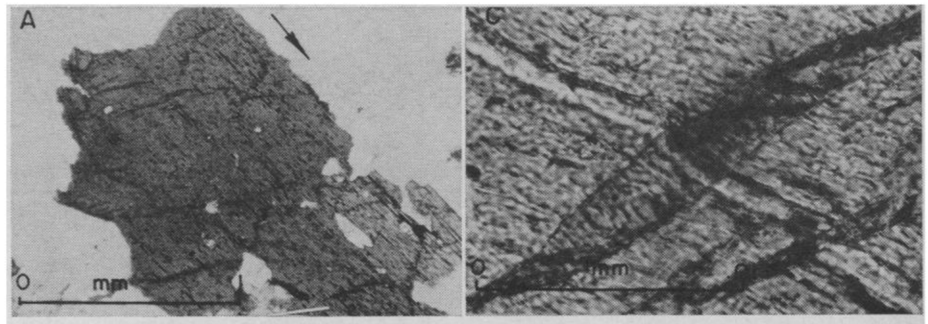

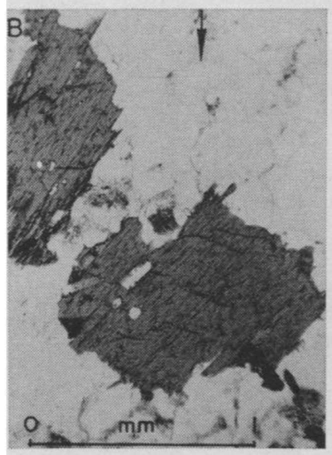

Fig. 2. Photomicrographs (plane polarized light) showing kink-bands in biotite. Arrows indicate stress direction (shock-wave propagation). Thin sections from core samples C_{10} and C_{11} used for photographs have known orientations with respect to the shot point. *A*, Kink-bands developed normal to stress direction. Crystallographic orientation of biotite with respect to the plane of the thin section is almost parallel to (001). The small black lines in the biotite almost parallel to direction of stress are inclusions. *B*, Kink-bands developed normal to stress direction (upper left and left center), at 50° (left center), and 70° (center). Other kink-bands are developed between 10° and 30° (center). Crystallographic orientation with respect to the plane of the thin section of both biotite grains is almost perpendicular to (001). Examination of thin sections prior to shot revealed no kink-bands and no apparent preferred orientation of biotite grains. *C*, Higher magnification photomicrograph of upper portion of *A* showing details of kink-bands.

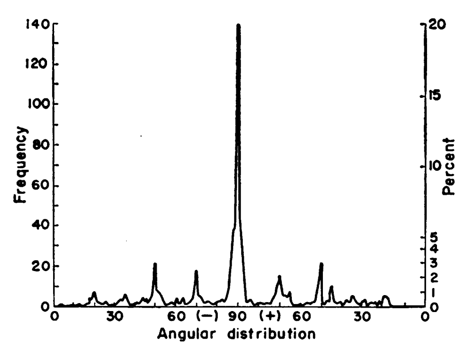

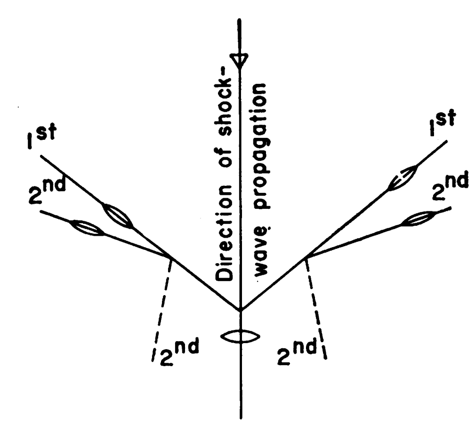

Fig. 3 (left). Frequency distribution of kink-band orientations with respect to dominant orientation. The dominant kink-band orientation, based on 110 measurements from oriented sections, is at 90° to the direction of shock-wave propagation. Kink-bands making angles in a counterclockwise direction with respect to the dominant orientation are plotted as (+); those making angles in a clockwise direction with respect to the dominant orientation are plotted as (−). Fig. 4 (right). Theoretical directions of first- and second-order shears with respect to the direction of stress (shock-wave propagation) (*6*). Dominant set of kink-bands is formed normal to the direction of shock-wave propagation. Observed concentrations of kink-band orientations interpreted as shear are indicated by solid lines. Although four directions of second-order shearing are possible, only two are present. Dashed lines indicate undeveloped shear directions. Kink-band orientations with respect to direction of shock-wave propagation and shear directions are indicated by shape of lens.

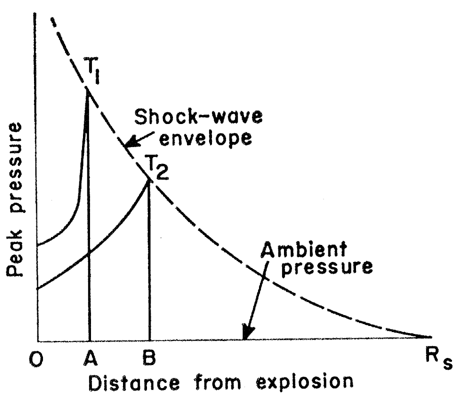

Fig. 5. Diagram of shock-wave propagation (*8*).

and magnitude to reorient the local stress field, thereby creating the second-order shears required to develop the 70° concentrations.

There does not seem to be a relation between the formation of kink-bands and the relation of the direction of the crystallographic axes of the biotite to the direction of shock-wave propagation. Whereas previous workers (*2*) suggested that kink-bands tended to develop preferentially in grains whose [001] axes [that is, normals to (001)] are steeply inclined to the compression axis, the present work indicates no such preference. Rather, in the shock zone of a nuclear explosion, kink-bands in biotite can be formed almost without regard to the crystallographic orientation. One difference in the conditions of the laboratory experiment (*2*) and the nuclear explosion which may account for the indiscriminate development of kink-bands with respect to the crystallographic axes is that the stress produced by the nuclear explosion's shock wave is of such a large magnitude and rapid application that the crystallographic anisotropy of biotite has little influence on kink-band formation.

The mode of failure, under the extremely rapid dynamic loading of a shock wave from a nuclear explosion, may be quite different from the mode of failure under the essentially static loading applied in laboratory experiments. The mode of failure, therefore, may not follow the same preferred crystallographic orientation under shock loading as under static loading.

DAVID CUMMINGS*

U.S. Geological Survey, Denver, Colorado

References and Notes

1. The radius of the shock zone for the granodiorite, R_s, may be obtained by using the scaling formula $R_s = 75\ W^{1/3}$, where W is the yield of the nuclear explosive in terms of trinitrotoluene equivalents.
2. D. T. Griggs, F. J. Turner, H. C. Heard, *Geol. Soc. Am. Mem.* **79**, 65 (1960).
3. M. S. Paterson and L. E. Weiss, *Nature* **198**, 1046 (1962).
4. J. G. Ramsey, *Geol. Mag.* **99**, 516 (1962).
5. H. E. McKinstry, *Am. J. Sci.* **251**, 401 (1953).
6. J. D. Moody and M. J. Hill, *Bull. Geol. Soc. Am.* **67**, 1207 (1956).
7. "Mathematically, a shock wave is an actual discontinuity propagating with a velocity greater than the local sound velocity," E. H. Freedman and E. F. Green, in *American Institute of Physics Handbook*, D. E. Gray, Ed. (McGraw-Hill, New York, 1957), pp. 2–231.
8. S. Glasstone, Ed., *The Effects of Nuclear Weapons* (U.S. Atomic Energy Commission, Washington, D.C., 1962), p. 104.

9. Work done on behalf of the U.S. Atomic Energy Commission. Publication authorized by the Director, U.S. Geological Survey. I thank the Lawrence Radiation Laboratory for providing the core samples.

* Present address: Astrogeological Branch, U.S. Geological Survey, Flagstaff, Arizona.

8 February 1964

Growth Layers on Ammonium Dihydrogen Phosphate

Abstract. *Microscopic observations of growth layers and etch pits on ammonium dihydrogen phosphate crystals reveal screw dislocations on the {100} face generating elliptical spirals that change rapidly but reversibly to rectangular shape when chromium-ion impurity is added. The effects of the impurity on crystal habit are judged to be secondary to changes in the morphology of the growth layers. No sources of growth are observed on the {101} faces; the layers spread inward from the edges and at times are mutually annihilating so that, temporarily, no steps are observed. Similar behavior is recorded for the* $\{10\bar{1}1\}$ *faces of* $NaNO_3$.

Bunn and Emmett (*1*) stimulated interest in the formation of growth layers at the same time that Frank (*2*) suggested that crystal dislocations could provide the sources of steps required for continuous crystal growth. Albon and Dunning (*3*) developed a particularly fine experimental technique for the observation of layer morphology and growth kinetics of sucrose. Their methods have been emulated and extended in our investigation of the mechanism of growth of ammonium dihydrogen phosphate crystals from aqueous solution. In particular, we studied the nature of the deposition process itself, whether by surface nucleation or as initiated at dislocation sites, and as influenced by impurities.

In experiments with crystals that are nucleated more readily than sucrose, the chief difficulty arises from the occurrence of spontaneous growth in tubes connecting the storage vessel to the growth cell. Undue heating of these leads necessarily interferes with precise temperature control in the cell.

The crystals were grown in a thin (3-mm) cell consisting of top and bottom (black) glass plates of optical quality, secured in a gold-plated brass block. Inlet and outlet tubes allowed the circulation of salt solution from an external, carefully lagged, storage thermostat (40°C) by means of a variable peristaltic pump. Housed in a poly(methyl methacrylate) container, the cell could be rotated about the axis of the microscope tube and given some degree of tilt so that a particular face of a crystal could be brought into position to be strongly illuminated by a focused beam of light. Photomicrographs were taken with a 35-mm single-lens reflex camera and with fine-grain film. For cine-film recording we used a 16-mm camera and reversal film.

Heat was supplied to or withdrawn from the growth cell by means of a Peltier junction attached to the bottom of the cell. Thus the temperature of the cell could be raised or lowered to increase super- or undersaturation as desired. While unintentional temperature fluctuations in the cell block amounted to a few thousandths of a degree Celsius, as measured with a platinum resistance thermometer, it was suspected that fluctuations in the solutions tended to be somewhat greater.

We found that growth on the {100} face of ammonium dihydrogen phosphate crystals proceeds by a screw dislocation mechanism. The spirals are roughly elliptical in shape (eccentricity about 0.86) and oriented with the short axis of the ellipse parallel to the [001] axis of the crystal. Growth proceeds by the movement of steps across the crystal face. The steps are of varying height, visibility being roughly proportional to the step height. Occasionally we found single spirals as in Fig. 1. However, most frequently